HFT-T, a Targeting Nanoparticle, Enhances Specific Delivery of Paclitaxel to Folate Receptor-Positive Tumors

Dong M. Shin *et al*.

Winship Cancer Institute,

Emory University School of Medicine,

Weill Medical College of Cornell University,

Emory University Rollins School of Public Health,

Habeeb Muhammed M. A.

26-09-09

INTRODUCTION

Paclitaxel is a chemotherapeutic agent for the treatment of advanced solid carcinomas, such as breast, ovaries, lung, and head and neck.

Utility of paclitaxel is compromised by its poor aqueous solubility that necessitates its formulation with the surfactant Cremophor EL as a delivery vehicle, which can cause serious side effects including allergic reaction, nephrotoxicity, neurotoxicity, and cardiotoxity.

A novel targeted polymeric ternary nanoparticle (HFT-T), which is composed of heparin-folate-paclitaxel (HFT) conjugates loaded with paclitaxel (T) in its hydrophobic core is developed. HFT-T exhibits improved water solubility, stability, biodegradability, and tunable drug loading capacities.

Folic acid (FA) is chosen as a targeting agent.

Natural polymer heparin, a commonly used carrier for growth factor delivery is used to synthesize HFT-T. Heparin improves response and survival in cancer patients taking chemotherapy, and has an inhibitory effect on tumors.

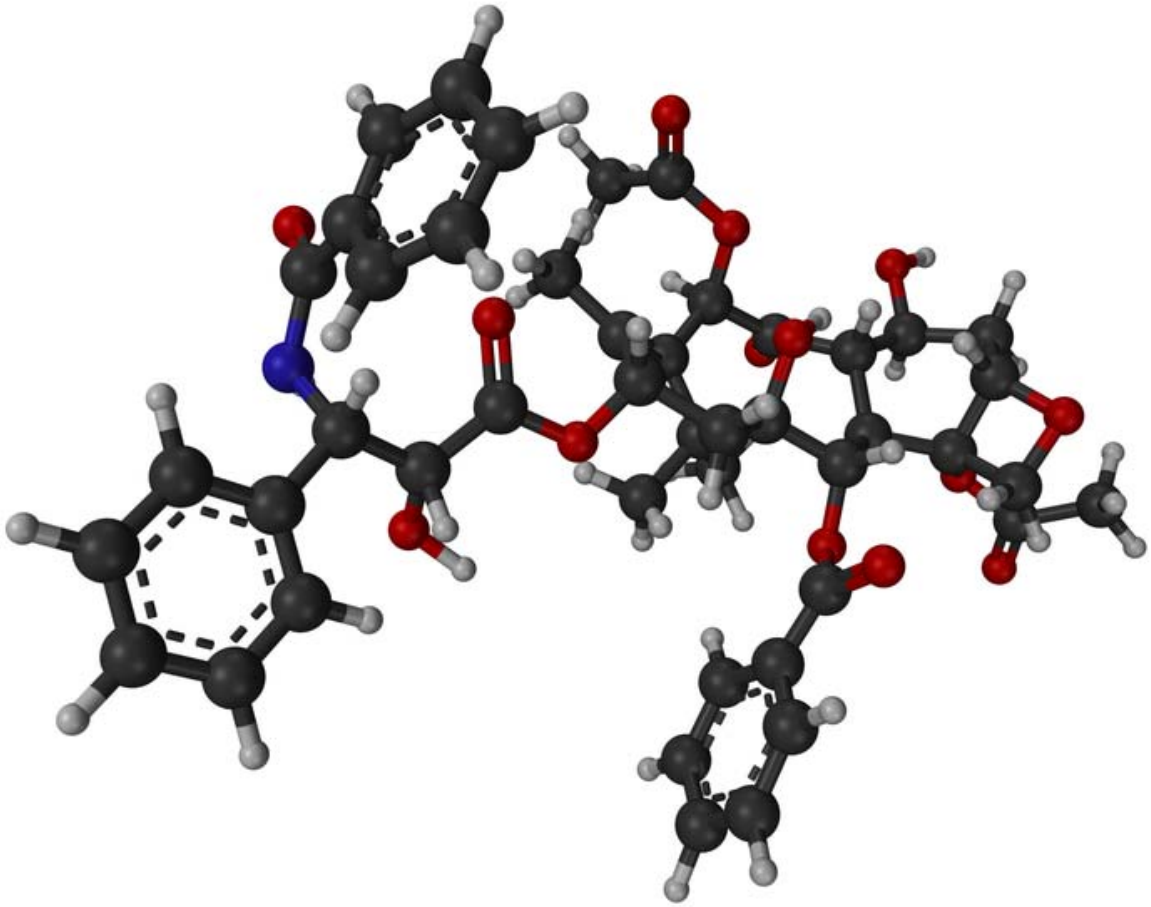

3D Chemical structure of Paclitaxel

Abstract

A ternary nanoparticle heparin-folic acid-paclitaxel (HFT), loaded with additional paclitaxel (T) was synthesized.

HFT-T retains the antitumor activity of paclitaxel and specifically target folate receptor (FR)-expressing tumors, thereby increasing the bioavailability and efficacy of paclitaxel.

In vitro experiments found that HFT-T selectively recognizes FR-positive human head and neck cancer cell line KB-3-1, displaying higher cytotoxicity compared to the free form of paclitaxel.

In a subcutaneous KB-3-1 xenograft model, HFT-T administration enhanced the specific delivery of paclitaxel into tumor tissues and remarkably improved antitumor efficacy of paclitaxel.

Paclitaxel tumors showed a resurgence of growth after several weeks of treatment, but this was not observed with HFT-T.

This indicates that HFT-T could be more effective in preventing tumors from developing drug resistance. No significant acute *in vivo toxicity was* observed.

These results indicate that specific delivery of paclitaxel with a ternary structured nanoparticle (HFT-T) targeting FR-positive tumor is a promising strategy to enhance chemotherapy efficacy and minimize adverse effects.

Result and discussion

Two types of nanoparticles were synthesized and compared with free paclitaxel

1. Binary nanoparticle- HT (heparin-paclitaxel)-no targeting agent

2. Ternary nanoparticle- HFT (heparin-folic acid- paclitaxel)-with targeting agent

Paclitaxel was conjugated onto the heparin backbone through the ester linker to yield HT. For HFT synthesis, ethylene diamine-modified folic acid was conjugated onto heparin through the amide linker.

The content of paclitaxel and folate in HFT was 15% and 9% (w/w), respectively. To increase the loading ratio of paclitaxel, free paclitaxel was incorporated into the HT and HFT conjugates to form nanostructures (HT-T and HFT-T) by a self-assembly procedure with an efficiency above 90%. The paclitaxel content of HFT-T was increased to 26% (w/w).

Transmission electron microscopy (TEM) showed that HFT-T nanoparticles were monodisperse, highly soluble, and stable in aqueous solution . The dynamic size of HFT-T nanoparticles measured by dynamic light scattering (DLS) was 60 nm.

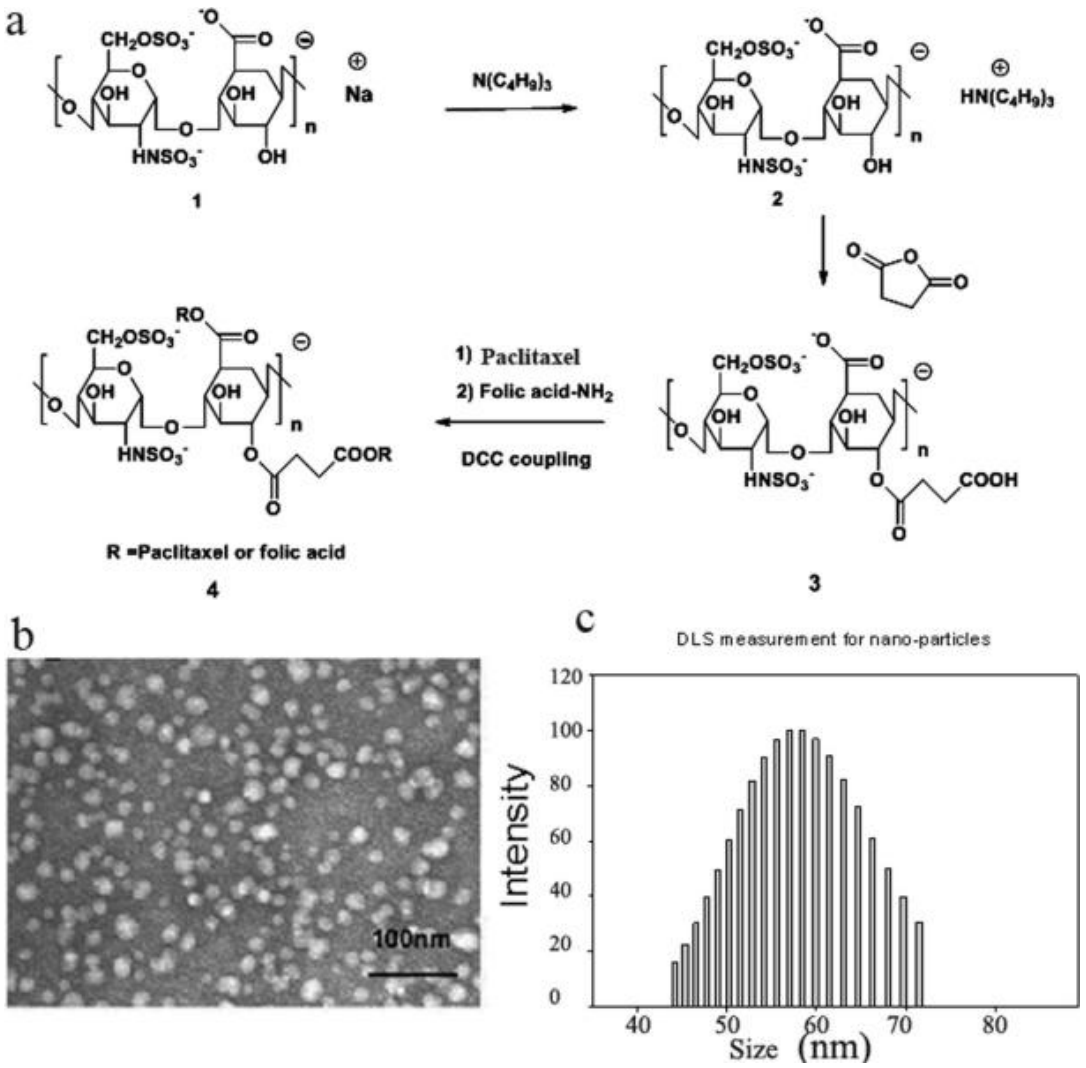

Figure 1. Synthesis and characterization of heparinfolic acidpaclitaxel nanoparticles loaded with paclitaxel (HFT-T): (a) diagram of conjugation reaction for heparinfolic acidpaclitaxel (HFT) conjugate; (b) TEM image of HFT-T nanoparticles; (c) DLS measurement of HFT-T nanoparticles; the graph shows size distribution of HFT-T nanoparticles in water.

In Vitro Cytotoxicity of HFT-T

Cytotoxic activity of free paclitaxel , HT-T and HFT-T nanoparticles were compared.

A colony formation assay was performed using the human head and neck cancer cell lines KB-3-1 (with folic acid receptor) and Tu212 (no folic acid receptor).

Cells were exposed to 2.5 nM paclitaxel and the HFT-T and HT-T nanoparticles at a paclitaxel-equivalent dose of 2.5 nM.

In KB-3-1 cells, after two weeks of incubation, treatment with free paclitaxel and HT-T reduced colony formation by 50% as compared with the untreated control, while HFT-T treatment reduced colony formation by 95% when compared with the control. This indicates that HFT-T has increased cytotoxicity in vitro.

In contrast, HFT-T showed a similar inhibitory effect in FR-negative Tu212 cells as compared to HT-T or free paclitaxel treatment .

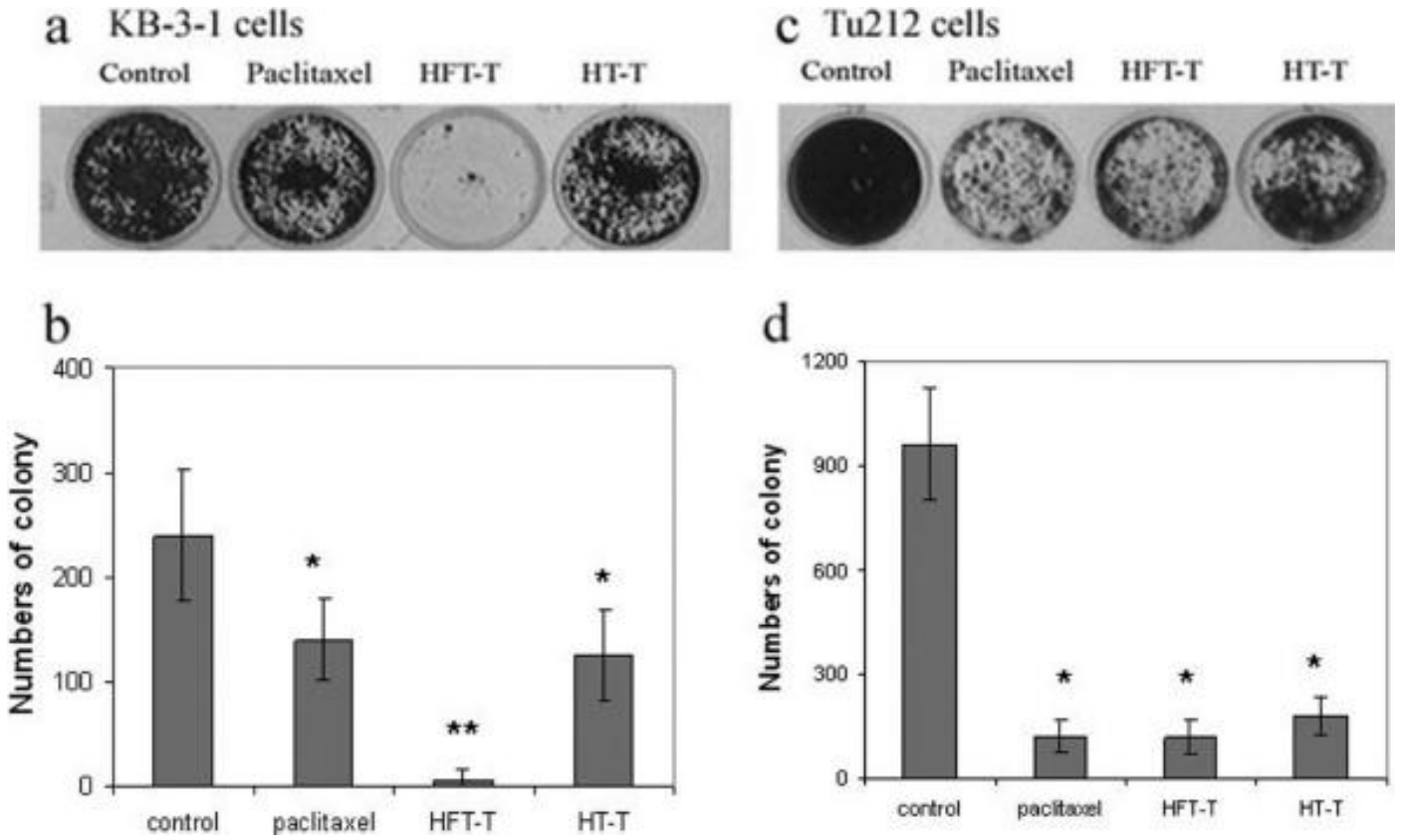

Figure 2. Effect of HFT-T on colony formation. KB-3-1 (a,b) and Tu212 (c,d) cells were treated with 2.5 nM paclitaxel or paclitaxel-equivalent dose of HFT-T or HT-T for 2 weeks. Colony-forming capability was markedly suppressed by HFT-T treatment when compared with all other treatments in KB-3-1 cells, but was similar in Tu212 cells. (**p0.05 and **p0.001 compared* with control, results are mean SE).

Specific *in Vitro Binding and Internalization of HFT-T*

Uptake of HFT-T and HT-T by KB- 3-1 cells was compared.

Confocal microscopy indicated that HFT-T underwent greater cellular uptake than HT-T. The level of nanoparticle internalized in KB-3-1 cells was quantified by flow cytometry and found to be five times greater in HFT-T-treated than HT-T-treated cells.

To assess the specificity of FR targeting, FR-specific siRNA was used to reduce FR levels. HFT-T cellular uptake was decreased.

In FR-negative Tu212 cells, HFT-T cellular uptake was less than that in FR-positive KB-3-1 cells.

In live-cell analysis, double fluorescence staining of HFT-T (paclitaxel-oregon green 488) and endosomes/ lysosomes (LysoTracker Red DND-99) was performed to visualize the intracellular distribution of HFT-T. The majority of HFT-T was observed in endosomes/lysosomes after 2 h of incubation, as evidenced by colocalization of green fluorescence from HFT-T and red fluorescence from LysoTracker .

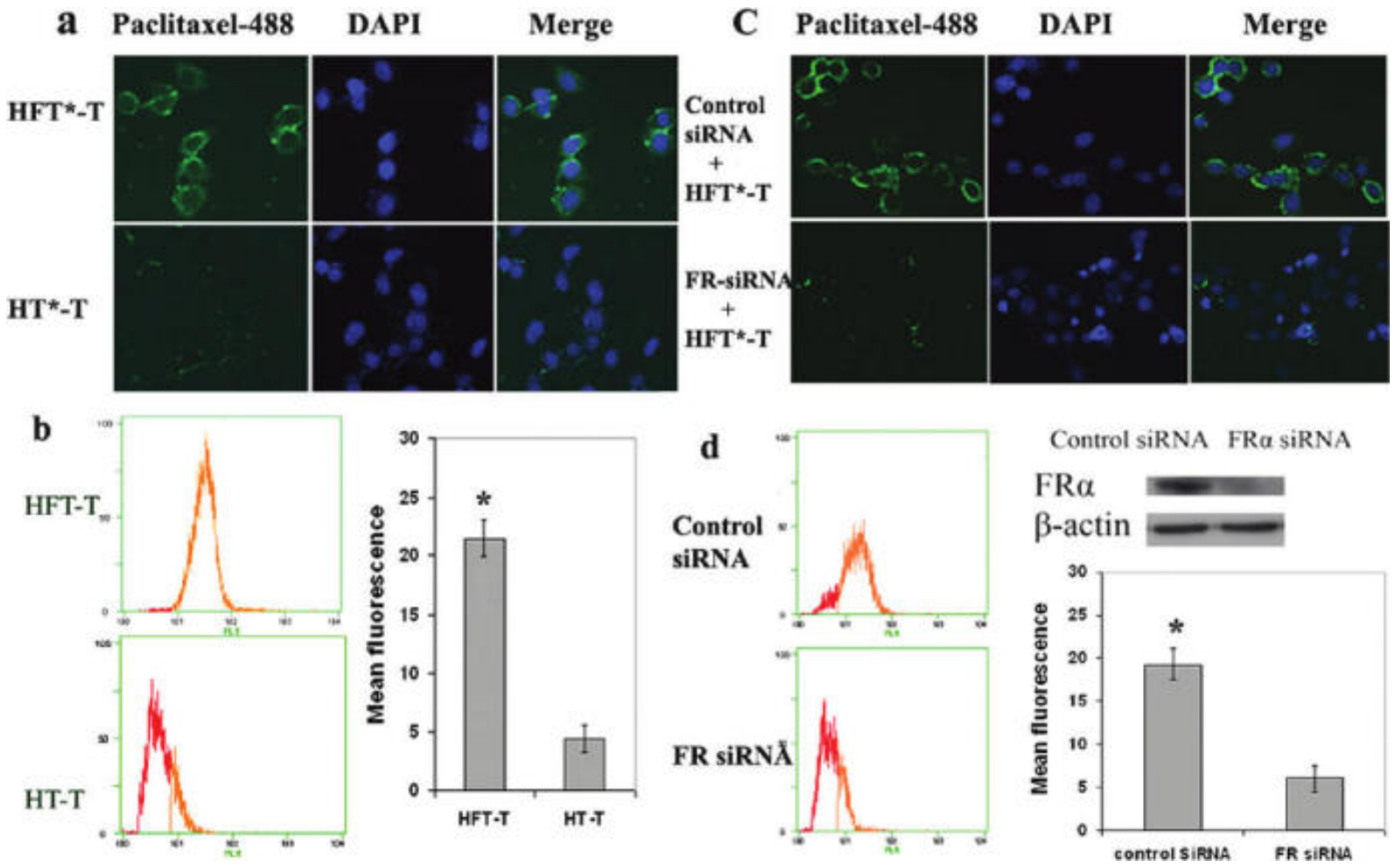

Figure 3. Specificity of tumor cell targeting of HFT-T. (a) Confocal images show KB-3-1 cell uptake of HFT-T or HT-T after 2 h incubation. (b) Uptake of HFT-T or HT-T by KB-3-1 cells was evaluated by flow cytometry. Left panel shows the mean fluorescence in cells after 2 h exposure to HFT-T or HT-T at 37 °C. (c) Confocal images show that the uptake of HFT-T in KB-3-1 cells treated with FR siRNA (FR-knockout) was decreased compared with that in KB-3-1 cells treated with the control siRNA. (d) Immunoblotting analysis was used to examine level of FR protein in KB-3-1 cells after treatment with the siRNA for FR or control siRNA. Uptake of HFT-T by FR knockout KB-3-1 cells or control KB-3-1 cells was analyzed by flow cytometry. (*p 0.05, results are mean SE).

Accumulation of HFT-T in Xenograft Tumors

To compare the *in vivo distribution of HFT-T and HT-T,* near-infrared dye (Cy5.5)-labeled HFT-T and HT-T nanoparticles were prepared, which provided real-time imaging of their *in vivo biodistribution in mice after systemic injection* through the tail vein.

Imaging of mice demonstrated tumor accumulation of both HFT-T and HT-T 1, 24, and 48 h after the injection. A fluorescence signal was also observed in the bladder 148 h after the injection. This signal was likely caused by small dye molecules cleaved from the nanoparticles and/or from heparin-dye conjugates that were dissociated from the particles.

Forty-eight hours after injection, the liver, kidney, lung, heart, and spleen were collected, and all tissues were analyzed by fluorescence imaging. For both HFT-T and HT-T, the greatest fluorescence intensity was observed in the tumor compared with the other tissues. Although the signal intensity in tumor tissue was slightly higher for HFT-T than HT-T, the difference was not significant.

To check whether HFT-T and HT-T nanoparticles simply accumulate around the tumor sites (outside the tumor cells) or actually enter the cells fluorescent dye (paclitaxel-bodipy 564)-labeled HFT-T or HT-T was injected through the tail vein of nude mice bearing KB-3-1 tumors.

Twenty-four hours post injection, tumors were harvested and the cellular uptake of HFT-T or HT-T was evaluated by staining with antihuman CD326 (EpCAM) antibody to distinguish human carcinoma cells from the host/murine stromal cells.

Fluorescence microscopy showed that fluorescent dye-labeled HFT-T predominantly accumulated within the tumor cells while HT-T was found predominantly in the extracellular space.

These data demonstrated that the specific FR-targeted nanoparticle, HFT-T, more efficiently delivered anticancer drug into tumor cells than the nontargeted nanoparticle, HT-T.

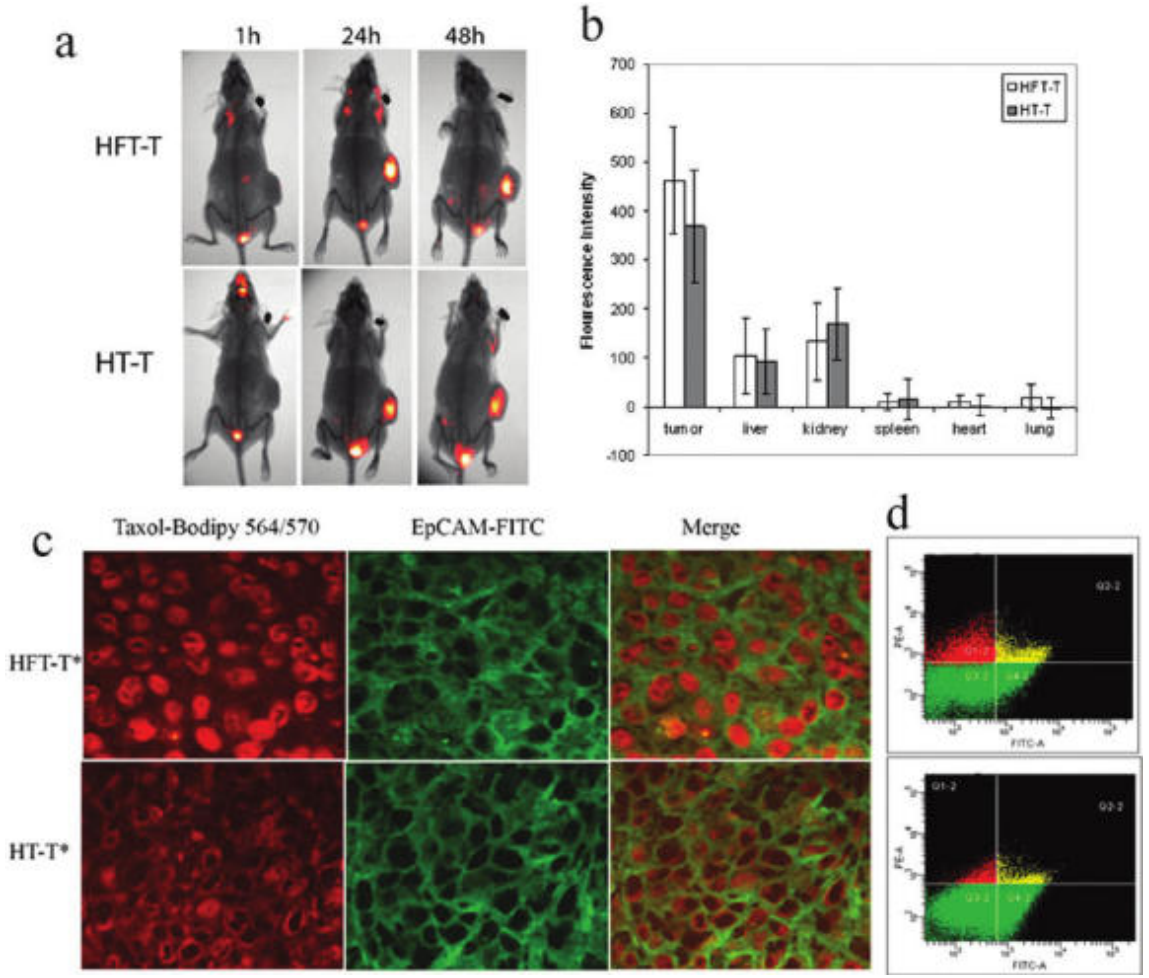

Figure 4. *In vivo distribution of HFT-T in KB-3-1 tumor-bearing mice. Near infrared dye (cy5.5)-labeled* HFT-T or HT-T was injected *i.v. into KB-3-1 tumor-bearing mice. (a) Imaging of mice at 1, 24, and* 48 h after injection. (b) Biodistribution of HFT-T and HT-T in major organs at 48 h after injection. (c) The cellular internalization of HFT-T *versus HT-T in KB-3-1 xenografts 24 h after injection (i.v.). HFT-T* showed marked internalization in KB-3-1 cells identified by human EpCAM expression (green). In contrast, HT-T showed much less internalization by KB-3-1 cells and was predominantly found in the extracellular space. (d) Flow cytometry analyses of cells obtained from disaggregated KB-3-1 xenografts 24 h after *i.v. injection of HFT-T or HT-T. Two-dimensional event density plots of disaggregated* tumor cell suspensions from animals injected with HFT-T or HT-T. The cells were stained with anti-EpCAM Ab-FITC conjugate to identify human cancer cells. The cells in Q4-2 and Q2-2 were human tumor cells (EpCAM positive), the cells in Q1-2 and Q2-2 contained nanoparticles (bodipy 564 positive), and the cells in Q2-2 were human tumor cells containing nanoparticles (double positive).

In Vivo Antitumor Efficacy and Toxicity of HFT-T

The efficacy of the HFT-T nanoparticles in promoting regression of pre-established tumors in a KB-3-1 xenograft model was evaluated.

Tumor-bearing mice were divided into four groups *in a way to minimize* weight and tumor size differences among the groups: control group (saline), free paclitaxel group (20 mg/kg), HT-T group, and HFT-T group (20 mg/kg paclitaxel equivalent for nanoparticles).

Therapy was continued once per week through tail vein injection for 5 weeks (injection time: day 1, 7, 13, 20, and 27).

All mice in the control group were sacrificed at day 15, earlier than those in the treatment groups, due to reaching the maximum tumor size according to the Institutional Animal Care and Use Committee (IACUC) guidelines.

After 5 weeks of treatment, all mice in the remaining treatment groups were sacrificed because some mice in the free paclitaxel and HT-T groups reached IACUC end-point volumes. Compared with the control group, tumor volumes in all treatment groups were significantly reduced *for free paclitaxel, HT-T, and HFT-T* each. Importantly, the tumor volume in the HFT-T-treated group was significantly smaller than that in the free paclitaxel *or HT-T-treated* groups, suggesting that the active targeting mechanism most likely contributes to the enhanced antitumor activity of HFT-T. Indeed, after five injections (at day 33 after first injection), the tumor volume in the HFT-T-treated group was only 5% of that in the free paclitaxel-treated group.

It was observed that while treatment with free paclitaxel suppressed tumor growth initially, after 3 weeks of treatment, tumors no longer responded to treatments and grew rapidly. This could have resulted from the tumor cells developing drug resistance to paclitaxel.

Unlike free paclitaxel, HFT-T did not show this resurgence in tumor growth rate after the same period of treatment. Three tumors in the HFT-T-treated group shrank to a non palpable size, leaving only scar tissue (by pathologic assessment), and these mice were cured, while no cures were attained in other treatment groups.

This is strong evidence that HFT-T is much more effective than free paclitaxel in treating tumors and is less susceptible to drug resistance, which is a very common occurrence in patients clinically treated with paclitaxel.

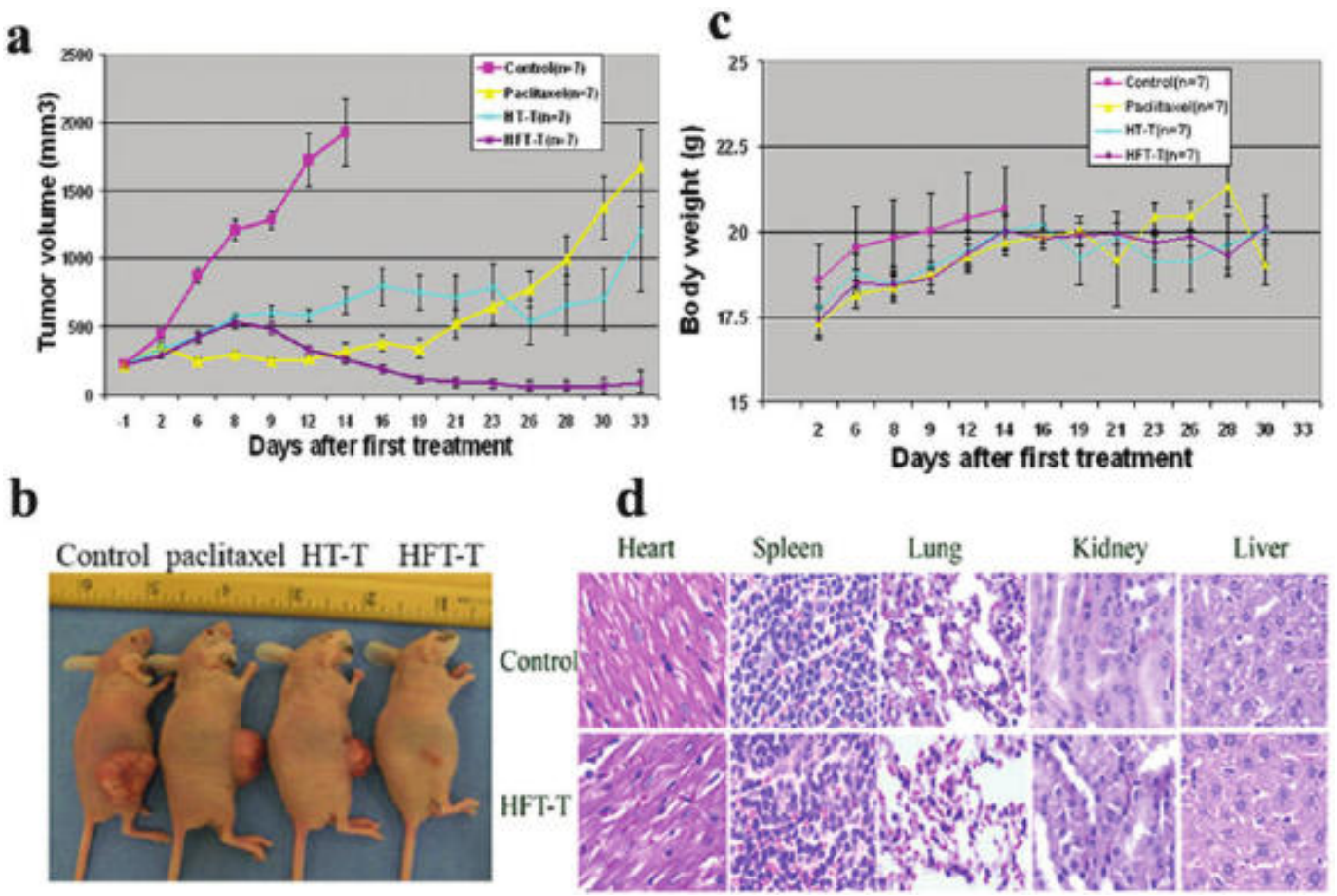

Antitumor effect of HFT-T nanoparticle in animal model. (a). The growth curve of KB-3-1 xenografts showed that all the treatment groups including free paclitaxel, HT-T, and HFT-T significantly inhibited the growth of tumor as compared with the control (*p 0.0001 for each treatment).* Although the tumor volumes were similar in HT-T and free paclitaxel-treated groups (*p 0.608), Frtargeted* HFT-T more potently reduced tumor growth than free paclitaxel (*p 0.0001). After five injections,* the average tumor volumes in paclitaxel, HT-T, and HFT-T treatment groups were 1670.3 286.1 mm3, 1211.3 448.1 mm3, and 92.9 78.2 mm3, respectively. (b) A representative mouse from each group. (c) The body weights of the mice in all groups. (d) Representative images of H&E organ staining from control and HFT-T-treated mice (magnification 200).

Systemic toxicity of free paclitaxel, HT-T, and HFT-T in the xenograft model was evaluated.

Compared with the control group, the body weights of mice in all three treatment groups were similar, indicating a negligible acute toxicity at this dose (20 mg/kg paclitaxel-equivalent).

At day 34 (after 5 weeks of treatment), the histopathologic changes in major organs, such as liver, spleen, kidney, heart, and lung, from the mice in all treatment groups were examined by hematoxylin and eosin (H&E) staining.

No tissue damage was observed in any organ sample collected from any treatment group, including HFT-T.

Although the accumulation of HFT-T and HT-T in the liver and kidney were relatively high, in this study no tissue damage was observed in any of the organ samples collected from any treatment group, including HFT-T and HT-T under the tested conditions.

The heparin polymer used to synthesize the nanoparticles is biodegradable, so that HFT-T and HT-T accumulated in the liver and kidney may be degraded and eliminated through the renal system. A fluorescent signal was continually observed in the bladder 48 h after injection of fluorescent dyelabeled HFT-T or HT-T, implying the degradation and elimination of nanoparticles.

CONCLUSIONS

In summary, this novel FR-targeted nanoparticle HFT-T significantly facilitated the specific delivery of paclitaxel to FR-positive tumor cells and demonstrated strongly enhanced *in vivo efficacy when compared with* free paclitaxel. This leads to the belief that using targeted nanoparticles as a specific and efficient drug delivery system is a promising strategy to treat human cancers and other diseases.